



Source amplitudes of volcano-seismic signals determined by the amplitude source location method as a quantitative measure of event size

Hiroyuki Kumagai^{a,b,*}, Rudy Lacson Jr.^c, Yuta Maeda^a, Melquiades S. Figueroa II^c, Tadashi Yamashina^d, Mario Ruiz^e, Pablo Palacios^e, Hugo Ortiz^e, Hugo Yepes^e

^a National Research Institute for Earth Science and Disaster Prevention, Tsukuba, Ibaraki 305-0006, Japan

^b Graduate School of Environmental Studies, Nagoya University, Nagoya, Aichi 464-8601, Japan

^c Philippine Institute of Volcanology and Seismology, C.P. Garcia Ave., U.P. Campus Diliman, Quezon City, Philippines

^d Kochi Earthquake Observatory, Faculty of Science, Kochi University, 2-17-47 Asakura-honmachi, Kochi, Kochi 780-8073, Japan

^e Instituto Geofísico, Escuela Politécnica Nacional, P.O. Box 17-01-2759, Quito, Ecuador

ARTICLE INFO

Article history:

Received 19 December 2012

Accepted 1 March 2013

Available online 14 March 2013

Keywords:

Source amplitude

Scattering

Isotropic radiation

Magnitude

Scaling relation

ABSTRACT

The amplitude source location (ASL) method, which uses high-frequency amplitudes under the assumption of isotropic S-wave radiation, has been shown to be useful for locating the sources of various types of volcano-seismic signals. We tested the ASL method by using synthetic seismograms and examined the source amplitudes determined by this method for various types of volcano-seismic signals observed at different volcanoes. Our synthetic tests indicated that, although ASL results are not strongly influenced by velocity structure and noise, they do depend on site amplification factors at individual stations. We first applied the ASL method to volcano-tectonic (VT) earthquakes at Taal volcano, Philippines. Our ASL results for the largest VT earthquake showed that a frequency range of 7–12 Hz and a Q value of 50 were appropriate for the source location determination. Using these values, we systematically estimated source locations and amplitudes of VT earthquakes at Taal. We next applied the ASL method to long-period events at Cotopaxi volcano and to explosions at Tungurahua volcano in Ecuador. We proposed a practical approach to minimize the effects of site amplifications among different volcano seismic networks, and compared the source amplitudes of these various volcano-seismic events with their seismic magnitudes. We found a proportional relation between seismic magnitude and the logarithm of the source amplitude. The ASL method can be used to determine source locations of small events for which onset measurements are difficult, and thus can estimate the sizes of events over a wider range of sizes compared with conventional hypocenter determination approaches. Previously, there has been no parameter widely used to quantify the sources of volcano-seismic signals. This study showed that the source amplitude determined by the ASL method may be a useful quantitative measure of volcano-seismic event size.

© 2013 Elsevier B.V. All rights reserved.

1. Introduction

Seismic signals at volcanoes, including long-period (LP) and very-long-period (VLP) events, tremor, and volcano-tectonic (VT) earthquakes, are generated by magmatic and hydrothermal activity, and thus contain information about internal dynamics and stress states of volcanoes (e.g., Chouet, 1996; Neuberg, 2000; McNutt, 2005; Kawakatsu and Yamamoto, 2007; Zobin, 2012; Chouet and Matoza, 2013). Source location and event size are fundamental parameters used to characterize volcano-seismic signals, and their rapid and correct determination is critically important in volcano monitoring. However, it is often difficult or impossible to locate these signals by

conducting traditional hypocenter determinations, because onsets of typical LP events and tremor are emergent and those of VT earthquakes are masked by the relatively large ambient noise at volcanoes. Because of the difficulty of source location determination, the magnitudes of the events usually cannot be reliably determined. Although the reduced displacement (Aki and Koyanagi, 1981) has been used to estimate tremor source amplitudes, there is no widely used parameter to quantify the size of volcano-seismic events at different volcanoes.

Battaglia and Aki (2003) proposed the amplitude source location (ASL) method, which is based on a method originally proposed by Yamasato (1997). The ASL method assumes isotropic S-wave radiation and uses seismic amplitudes corrected for site amplifications. Kumagai et al. (2010) showed that the ASL method is useful to locate various volcano-seismic signals in a high frequency band around 5–12 Hz, including an LP event, an explosion event, and tremor associated with lahars and pyroclastic flows. They interpreted that the assumption of isotropic S-wave radiation is valid in this frequency band; the

* Corresponding author at: Graduate School of Environmental Studies, Nagoya University, Nagoya, Aichi 464-8601, Japan. Tel.: +81 52 789 3651; fax: +81 52 789 3013.
E-mail address: kumagai@eps.nagoya-u.ac.jp (H. Kumagai).

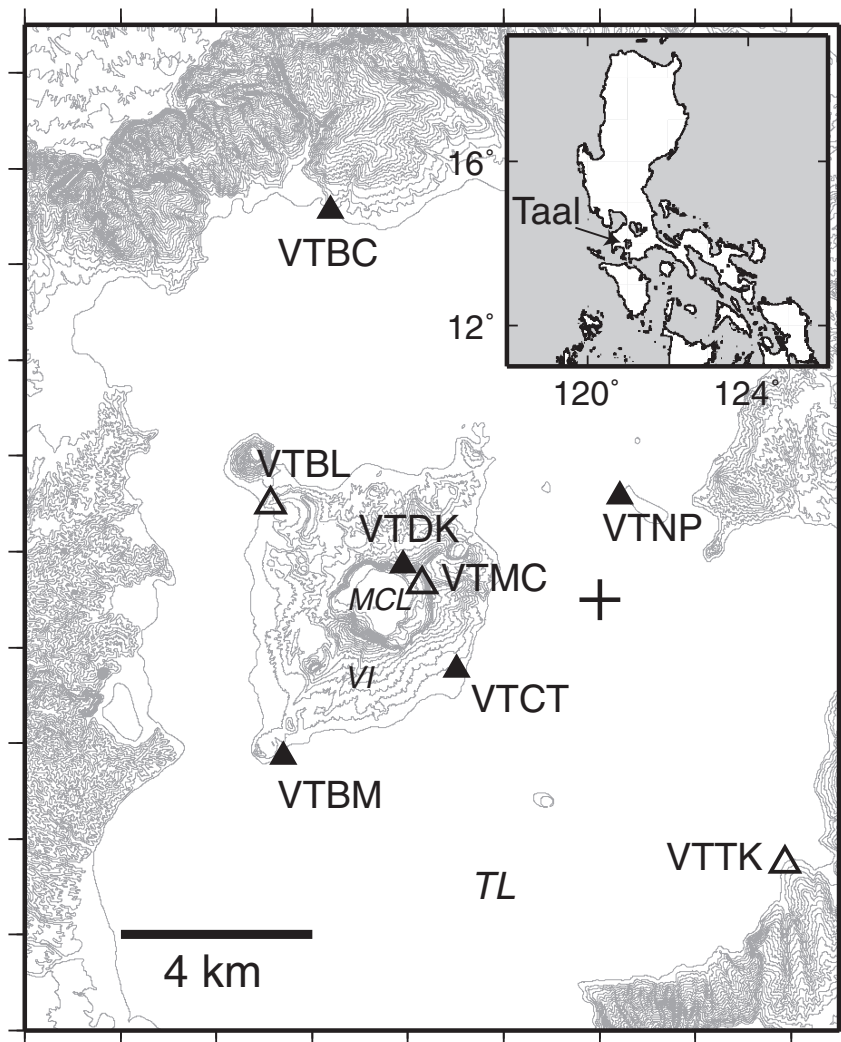


Fig. 1. Locations of broadband (solid triangles) and short-period (open triangles) seismic stations at Taal volcano, Philippines. The inset shows the location of Taal volcano. VI, Volcano Island; MCL, Main Crater Lake; TL, Taal Lake. The source location (plus sign) used to calculate the synthetic seismograms is at 3 km below sea level.

path effect caused by the scattering of seismic waves due to small-scale heterogeneities distorts the *S*-wave radiation pattern and results in isotropic *S*-wave radiation in a high frequency band. The frequency dependence of the *S*-wave radiation patterns of tectonic earthquakes was shown by Takemura et al. (2009). The validity of the assumption of isotropic *S*-wave radiation is supported by Kumagai et al. (2011b), who numerically simulated high-frequency seismic waveforms in heterogeneous media with volcano topography. Battaglia et al. (2003) used the ASL method to locate LP events beneath Kilauea volcano, Hawaii, and it has also been applied to the analysis of tremor signals at the Piton de la Fournaise volcano, Réunion Island (Battaglia et al., 2005a, 2005b) and at Meakandake, Japan (Ogiso and Yomogida, 2012). Kumagai et al. (2011a) also used the ASL method to analyze an explosion event at Tungurahua volcano, Ecuador.

One of the advantages of the ASL method over traditional hypocenter determination methods is that it can simultaneously determine the source location and the initial or source amplitude. It might be possible to use the source amplitude, defined as the amplitude at the source location calculated under the assumption of isotropic radiation of far-field *S* waves, as a quantitative measure of the size of an event producing volcano-seismic signals. Although Battaglia et al. (2005b) and Kumagai et al. (2011a) used the source amplitude to quantify tremor signals at the Piton de la Fournaise and an explosion event at Tungurahua, respectively, the source amplitudes of various volcano-seismic signals observed at different volcanoes have yet

to be systematically examined. Because the accuracy of the source amplitude estimate depends on the correct determination of the source location by the ASL method, the accuracy and resolution of source locations determined by this method must be examined. Furthermore, site amplification factors depending on a reference site should be carefully considered when comparing the source amplitudes at different volcanoes.

In this study, we first tested the ASL method at Taal volcano, Philippines by using synthetic seismograms for a network of eight seismic stations. As demonstrated by Kumagai et al. (2011b), extensive full waveform simulations using a highly heterogeneous structural model are required to reproduce high-frequency seismograms with isotropic radiation. Such extensive simulations, however, are beyond the scope of the present study. We therefore used Ricker wavelets assuming isotropic *S*-wave radiation for synthetic seismograms. Using

Table 1
One-dimensional *P*-wave velocity structure used in this study.

Depth (km)	<i>P</i> -wave velocity (m/s)
–1.0	3100
2.0	4300
4.0	4800
6.0	5200
8.0	6000
15.0	6000

these seismograms, we performed a series of tests to examine the effects of velocity structure, noise, and site amplification on ASL results. We then applied the ASL method to VT earthquakes at Taal, and compared the estimated source locations with hypocenters determined by using onset arrival times. We further applied the ASL method to LP events at Cotopaxi and explosion events at Tungurahua in Ecuador. We proposed a practical way of minimizing the effects of site amplifications to compare the source amplitudes estimated at different volcanoes. Our comparison of the source amplitudes of events at the three volcanoes showed that a scaling relationship exists between the source amplitude and seismic magnitude.

2. Method

We use the ASL method following Kumagai et al. (2010) and Kumagai et al. (2013). In this method, grid nodes are distributed in a three-dimensional search domain, and the far-field S-wave approximation is used. Then, the particle velocity v_{ij} at the i -th station from the j -th grid node may be written as

$$v_{ij}(t_s + \tau_{ij}) = A_0(\xi_j) s_0(t_s) \frac{1}{r_{ij}} e^{-C\tau_{ij}}, \tag{1}$$

where t_s is the source origin time; r_{ij} is the distance between station i and source node j ; τ_{ij} is the S-wave travelt ime from the j -th grid node to the i -th station; ξ_j is the location of the j -th grid node; and A_0 and s_0 are the radiation coefficient and the second time derivative of the moment function, respectively. Here, C is given by

$$C = \frac{\pi f}{Q}, \tag{2}$$

where f is frequency of an S wave and Q is the quality factor for medium attenuation. These equations, with a constant value of A_0 , represent isotropic S-wave radiation. We use sliding time windows for the source time t_s^k , defined as,

$$t_s^k = t_s + (k-1)T_w, \quad (k = 1, 2, 3, \dots), \tag{3}$$

where T_w is the window duration. The envelope amplitude averaged over the time window T_w is obtained from Eqs. (2) and (3) as follows:

$$g_{ij}(t_s^k + \tau_{ij}) = \frac{1}{T_w} \int_0^{T_w} \tilde{v}_{ij}(t + t_s^k + \tau_{ij}) dt, = A_{jk} \frac{1}{r_{ij}} e^{-C\tau_{ij}}. \tag{4}$$

Here, A_{jk} , which is the source amplitude at the j -th grid node and source time t_s^k , is given as

$$A_{jk} = \frac{1}{T_w} A_0(\xi_j) \int_0^{T_w} \tilde{s}_0(t + t_s^k) dt. \tag{5}$$

We can estimate the source amplitude A_{jk} by using the following equation,

$$A_{jk} = \frac{1}{N} \sum_{i=1}^N g_i^o(t_s^k + \tau_{ij}) r_{ij} e^{C\tau_{ij}}, \tag{6}$$

where N is the number of stations (see Appendix A). Here, $g_i^o(t)$ is the observed velocity envelope amplitude corrected for site amplification averaged over the time window T_w at the i -th station; $g_i^o(t)$ is given as

$$g_i^o(t_s^k + \tau_{ij}) = \frac{1}{T_w} \int_0^{T_w} \tilde{v}_i^o(t + t_s^k + \tau_{ij}) dt, \tag{7}$$

where $\tilde{v}_i^o(t)$ is the envelope of the observed velocity waveform $v_i^o(t)$. We correct the observed amplitudes by the coda normalization method (e.g., Phillips and Aki, 1986). To evaluate the fits between the observed

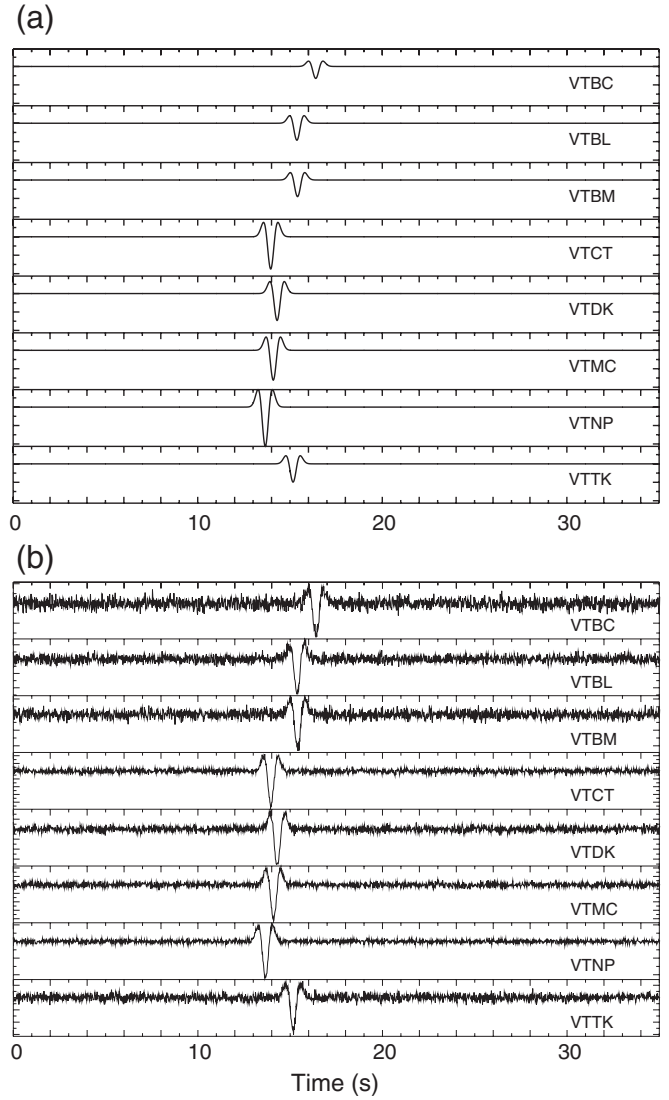


Fig. 2. Synthetic seismograms generated by assuming isotropic radiation of S waves and using a Ricker wavelet (a) without and (b) with added noise at the stations shown in Fig. 1. See the manuscript for details.

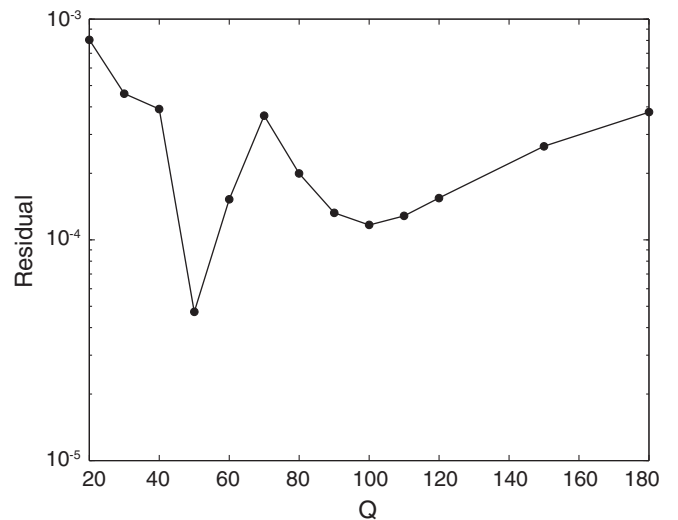


Fig. 3. Normalized residuals obtained from the ASL analysis of the synthetic seismograms in Fig. 2a as a function of Q .

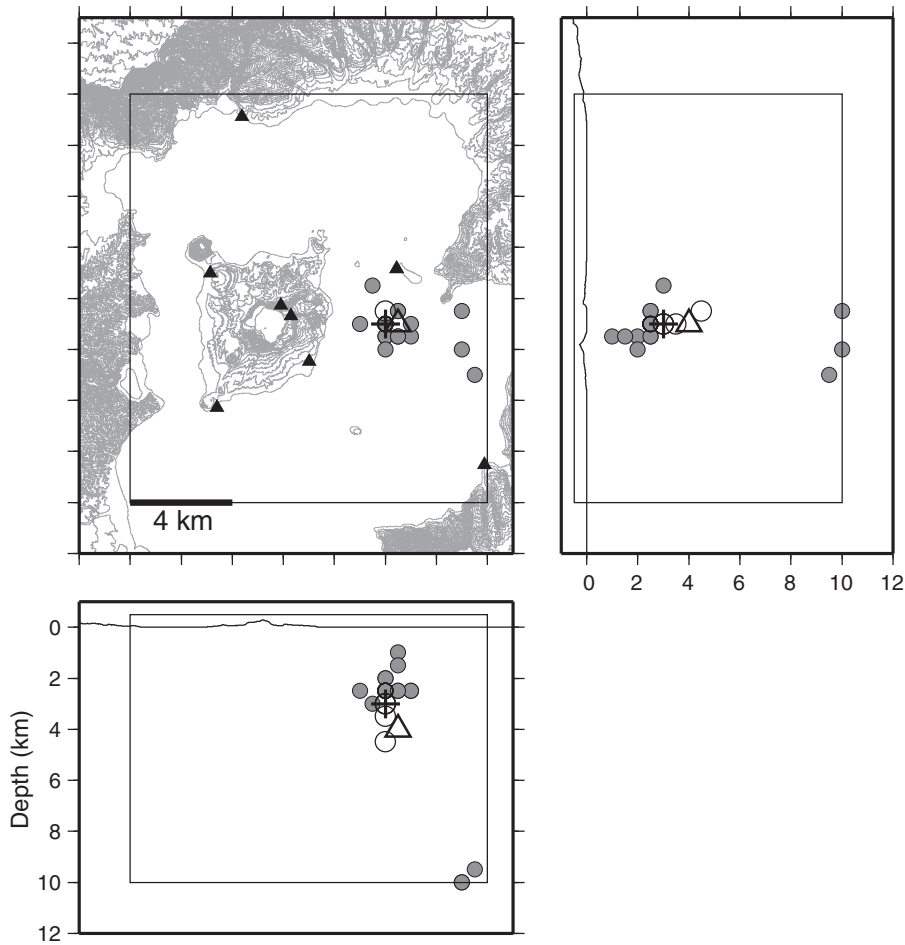


Fig. 4. Dependence of the source locations estimated with the ASL method from the synthetic seismograms in Fig. 2 on Q (open circles), noise (open triangle), and site amplification factors (gray circles). The plus sign indicates the input source location, and the solid triangles in the map view show the station locations. The region enclosed by solid gray lines in each panel represents the grid search domain.

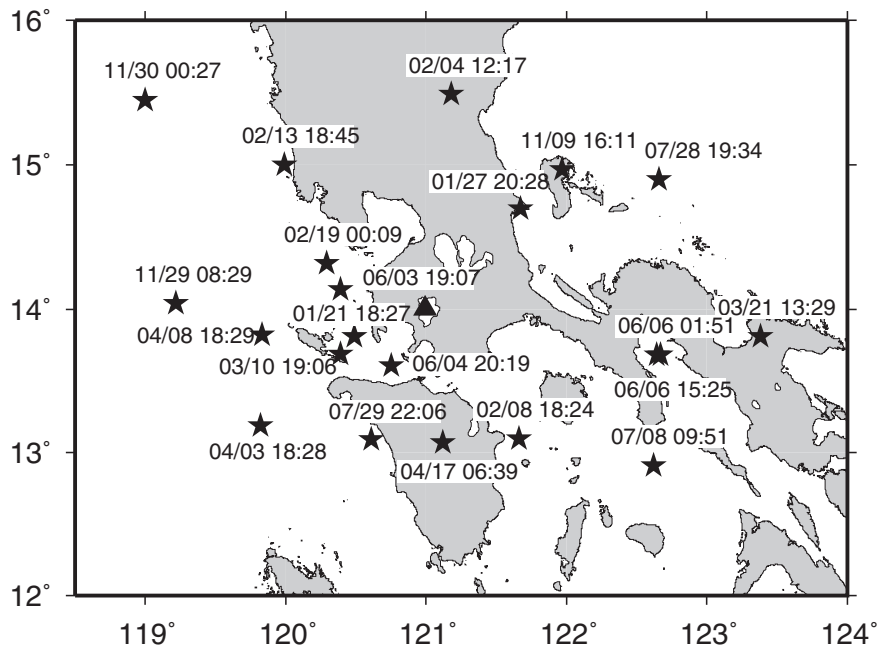


Fig. 5. Epicenters of tectonic earthquakes used in the coda normalization method to estimate site amplification factors at the stations shown in Fig. 1. The source depths of these earthquakes are shallower than 137 km.

Table 2

Site amplification factors and their standard errors in five frequency bands for the stations of the Taal seismic network relative to station VTNP.

Station	1–6 Hz	3–8 Hz	5–10 Hz	7–12 Hz	9–14 Hz
VTNP	1	1	1	1	1
VTBC	1.041 ± 0.088	1.249 ± 0.087	0.956 ± 0.102	0.703 ± 0.156	0.918 ± 0.302
VTCT	1.293 ± 0.117	0.817 ± 0.063	0.742 ± 0.171	0.801 ± 0.313	0.910 ± 0.428
VTTK	1.294 ± 0.092	1.104 ± 0.075	0.752 ± 0.065	0.609 ± 0.065	0.559 ± 0.088
VTBL	0.136 ± 0.010	0.095 ± 0.007	0.093 ± 0.007	0.087 ± 0.010	0.098 ± 0.013
VTDK	0.907 ± 0.079	1.161 ± 0.085	1.320 ± 0.180	0.940 ± 0.192	1.060 ± 0.332
VTBM	1.910 ± 0.158	1.044 ± 0.153	0.879 ± 0.106	0.944 ± 0.092	1.339 ± 0.240
VTMC	0.498 ± 0.025	0.608 ± 0.038	0.592 ± 0.107	0.703 ± 0.308	0.521 ± 0.307
Mean error percentage	7.7%	8.1%	13.4%	22.6%	31.0%

and calculated amplitudes in each time window, we use the normalized residual function E_{jk} , defined as

$$E_{jk} = \frac{\sum_{i=1}^N \{g_i^o(t_s^k + \tau_{ij}) - g_{ij}(t_s^k + \tau_{ij})\}^2}{\sum_{i=1}^N \{g_i^o(t_s^k + \tau_{ij})\}^2} \quad (8)$$

The minimum residual in each time window is found by a spatial grid search, and then the maximum A_{jk} in Eq. (6) among those estimated at the minimum residual positions in individual sliding time windows during an event is identified. We regard this maximum A_{jk} and its position as the event source amplitude and location, respectively.

3. Synthetic tests

In this section, we tested the ASL method using synthetic seismograms at Taal volcano, Philippines (Fig. 1), in which we examined the effects of Q , velocity structure, noise, and site amplification on ASL results. To calculate the synthetic seismograms, we used a Ricker wavelet defined by the following equation:

$$v(t) = \frac{\sqrt{\pi}}{2} (b^2(t) - 0.5) e^{-b^2(t)}, \quad (9)$$

where $b(t)$ is given by

$$b(t) = \pi(t - T_s)/T_p. \quad (10)$$

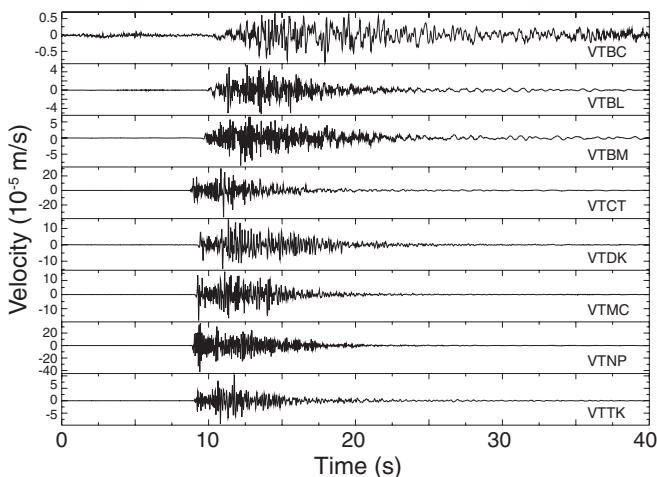


Fig. 6. Observed vertical seismograms of a VT earthquake on 31 May 2011 at Taal volcano.

Here, T_p and T_s are constants related to the duration and peak time of the wavelet. We calculated synthetic seismograms $v_{ij}(t)$ assuming isotropic far-field S waves by using the following equation:

$$v_{ij}(t) = v(t) \frac{1}{r_{ij}} e^{-C\tau_{ij}}, \quad (11)$$

where C is as given by Eq. (2). In our tests, we used the relation $T_s = 2T_p + \tau_{ij}$ and $f = 1/T_p$, and assumed $T_p = 1$ s and $Q = 50$. We used a

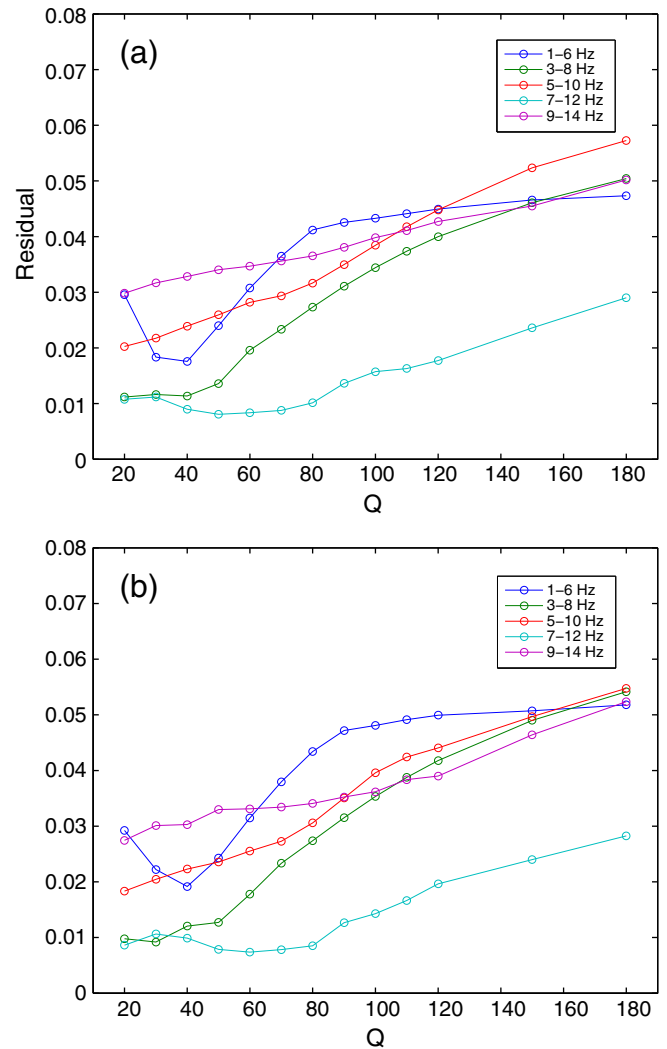


Fig. 7. Normalized residuals obtained by ASL analysis of the VT earthquake on 31 May 2011 (see Fig. 6) in different frequency bands as a function of assumed Q values. Traveltimes were calculated either (a) by using the 1D velocity model (Table 1) or (b) by assuming a homogeneous velocity structure with an S-wave velocity of 2500 m/s.

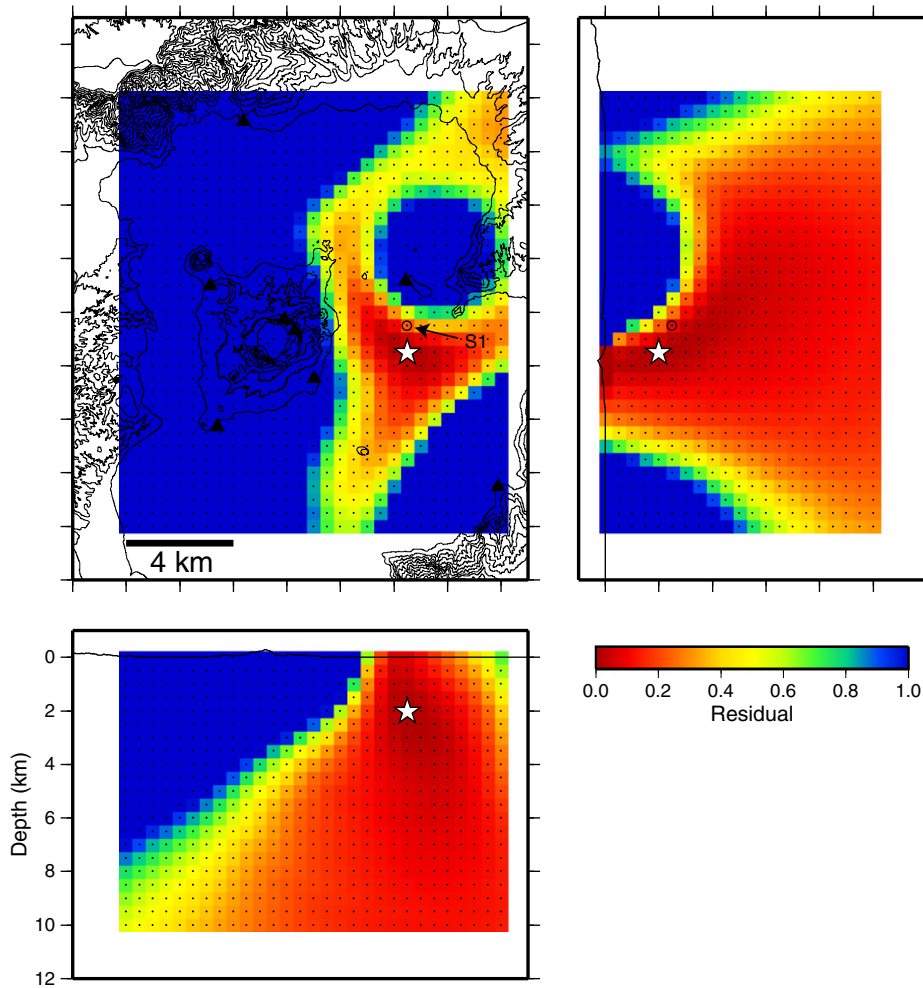


Fig. 8. Normalized residual distribution for the VT earthquake on 31 May 2011 (see Fig. 6) obtained by using a frequency band of 7–12 Hz, $Q = 50$, and 1D model traveltimes. Stars indicate the minimum residual location.

one-dimensional P -wave velocity model (Table 1), and calculated the S -wave traveltimes (τ_{ij}) by using the finite difference method based on the Eikonal equation (Vidale, 1990; Podvin and Lecomte, 1991; Benz et al., 1996). In our calculations of traveltimes, we assumed $\beta = \alpha/\sqrt{3}$, where α and β are P - and S -wave velocities, respectively. We used r_{ij} as the source-station distance rather than the ray length for simplicity.

To calculate the synthetic seismograms at eight stations at Taal (Fig. 2a), we used a source location (Fig. 1, plus sign) at a depth of 3 km below sea level. We applied the ASL method to these synthetic seismograms using a frequency band of 0.5–2 Hz, a time window between 10 and 20 s, traveltimes calculated with the one-dimensional model, and a grid search domain surrounding Taal with a grid interval of 500 m. We used various Q values between 20 and 180, and plotted the resultant minimum residual values (Fig. 3) and positions (Fig. 4, open circles). The minimum residual positions (open circles) were close to the input location (plus sign). The lowest value among these minimum residual values for this range of Q was obtained at $Q = 50$ (Fig. 3), and its source location was exactly the same as the input location.

We used traveltimes calculated with homogeneous velocity structures of $\beta = 2000$, 2500, and 3000 m/s and a Q value of 50, and performed an ASL analysis of the synthetic seismograms simulated with the 1D velocity model (Fig. 2a). For $\beta = 2000$ and 2500 m/s,

we obtained source locations that were exactly the same as the input location. For $\beta = 3000$ m/s, the source location was one grid node (500 m) deeper than the input location.

We next added random noise to the synthetic seismograms (Fig. 2b). The source location for these seismograms with added noise determined by using the 1D model traveltimes and $Q = 50$ was close to the input location (triangle in Fig. 4).

We then examined the effect of site amplification factors. Using uniform random numbers, we generated 15 sets of site amplification factors with variations of $\pm 20\%$ at each of the eight stations. The estimated source locations for the noise-free synthetic seismograms determined with these random amplification factors using 1D model traveltimes and $Q = 50$ (Fig. 4, gray circles) showed more scatters than the previous test results.

These test results indicate that ASL results are not strongly influenced by Q , velocity structure, or noise, but they are relatively more affected by site amplification factors.

4. Results

4.1. Observation network and site amplification factors at Taal volcano

Taal volcano is one of the most active volcanoes in the Philippines. It has erupted in 1977, and the subsequent dormant period has been

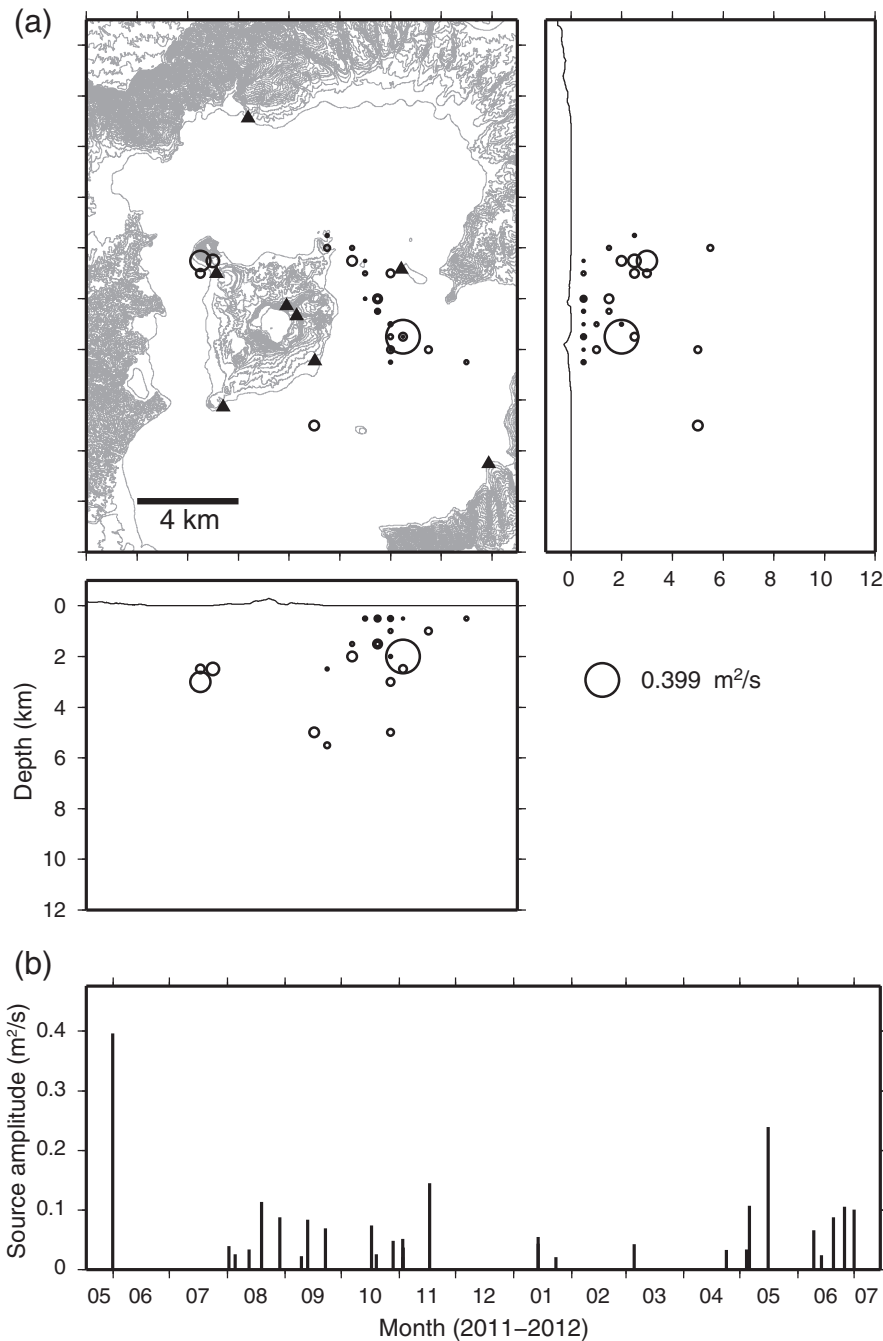


Fig. 9. (a) Source locations and source amplitudes of VT earthquakes at Taal volcano. The size of each circle indicates the source amplitude, which is scaled to a reference circle outside the map. (b) Source amplitudes as a function of time between May 2011 and July 2012.

exceptionally long. In November 2010, a joint Japan–Philippine team deployed a new multi-parameter observation network at Taal volcano consisting of seismic, electromagnetic, GPS, and infrasonic stations. This network is maintained by the Philippine Institute of Volcanology and Seismology (PHIVOLCS). These real-time data are transmitted to the head office of the PHIVOLCS in Metro Manila. The network includes five stations with broadband seismic sensors (Guralp CMG-40T, 0.02–60 s; VTBC, VTNP, VTDK, VTCT, and VTBM) and three with short-period seismic sensors (Kinematics SS-1, 1 s; VTMC, VTBL, and VTTK) (Fig. 1). Each broadband sensor was installed on a concrete base at a depth of 1–2 m below the ground surface and buried with sand. The short-period seismometer at each short-period station was installed on a concrete base above the ground surface inside a concrete house.

The seismic data are digitized by either a Kinematics K2 or a Basalt 24-bit data logger with a sampling frequency of 50 Hz.

We estimated site amplification factors for the individual stations by the coda normalization method (e.g., Phillips and Aki, 1986). Following Kumagai et al. (2010), we selected regional tectonic earthquakes with good azimuthal coverage (Fig. 5). We used envelopes of the vertical-component velocity seismograms of these earthquakes band-passed in five frequency bands (1–6, 3–8, 5–10, 7–12, and 9–14 Hz). In each envelope waveform, we used five 5-s windows that overlapped by 2.5 s starting from a lapse time that was twice the S-wave arrival time, and then averaged the mean amplitudes in the individual windows. We set VTNP as a reference station and estimated the site amplification factors (Table 2). In each frequency band,

the mean error percentage shown in Table 2 is the percentage error averaged over the seven stations (excepting the reference station). The mean error percentage increased with increasing frequency, suggesting that the estimation accuracy of the site amplification factors becomes worse as the frequency increases.

4.2. ASL analysis of VT earthquakes at Taal volcano

We first used the ASL method to estimate the source location of the largest VT earthquake during our observational period, which occurred on 31 May 2011 (Fig. 6). We applied band-pass filters in the five frequency bands to the observed vertical velocity waveforms, and obtained the envelopes of the band-passed waveforms. We then used a 10-s sliding time window with a 1-s overlap to estimate the mean amplitude of each waveform. We corrected the mean amplitudes by using the site amplification factors in the individual frequency bands. We performed grid searches using the five frequency bands and various Q values between 20 and 180, for which we used traveltimes calculated with the 1D velocity model or by assuming a homogenous S -wave velocity of 2500 m/s. We then plotted the resultant minimum residuals for each of the five frequency bands as a function of Q (Fig. 7). With both the 1D and homogeneous velocity models, the residuals were small in the 7–12 Hz frequency band. We obtained the global minimum residual at $Q = 50$ in the 7–12 Hz band with the 1D model traveltimes, and plotted the spatial distributions of the residuals in this band at $Q = 50$ (Fig. 8). The source location was determined in the southeastern part of Taal Lake at a depth of 2 km below sea level.

We then systematically estimated source locations and amplitudes of VT earthquakes that occurred beneath Taal after May 2011, when our automatic event triggering system was activated. We note that there are some ambiguities in the source amplitude estimations. The source amplitude depends on (1) the site amplification factors, which were determined as the coda amplitude ratios relative to those calculated at the reference station and (2) the frequency band used in the ASL method. These ambiguities may present problems for the comparison of source amplitudes of events at different volcanoes. Therefore, we estimated the source location and amplitude of each event by a two-step procedure. In step 1, we estimated the source location by using the observed amplitudes corrected for the site amplification factors in the 7–12 Hz band with $Q = 50$ and the 1D model traveltimes. Then, in step 2, assuming a reference frequency band of 5–10 Hz and $Q = 50$, we determined the source amplitude at the estimated source location by using observed envelope amplitudes only at broadband seismic stations, without performing any corrections for the site amplification factors. We set a reference frequency band of 5–10 Hz because this band was shown to be useful at other volcanoes (Battaglia and Aki, 2003; Kumagai et al., 2010) and may be used as the typical frequency band for the ASL method. Because the seismometers at the broadband stations at Taal were installed in the same way as those at Tungurahua and Cotopaxi volcanoes in Ecuador (Kumagai et al., 2010), we considered that the use of broadband data only would minimize station site effect differences among these three volcano networks. As shown in Table 2, the site amplification factors at the broadband stations in frequency bands of 5–10 and 7–12 Hz are close to unity, but those at short-period station VTBL show large deviations from unity. The factors at other short-period stations (VTTK and VTMC) also show relatively large deviations. These features support our assumption about the site effect. We also estimated the seismic magnitude (M_v) of each event using the relation of Watanabe (1971) given as

$$M_v = 1.18 \log v_{\max} + 2.04 \log r + 5.29, \quad (12)$$

where v_{\max} is the maximum vertical velocity amplitude (m/s) and r is the source-station distance in kilometers (<200 km). To minimize

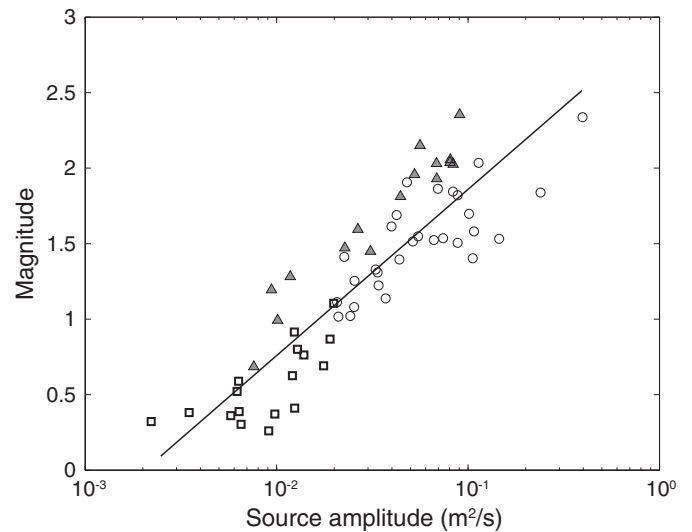


Fig. 10. Seismic magnitude versus the logarithm of the source amplitude for VT earthquakes at Taal volcano (open circles), LP events at Cotopaxi volcano (open squares), and explosion events at Tungurahua volcano (gray triangles). The solid line is the least squares fit to all data points (see Eq. (13)).

site effects in these seismic magnitude estimations, we also used only broadband seismic data. Because Watanabe (1971) derived this relation using data from a short-period seismic network, we applied a high-pass filter at 1 Hz to the vertical broadband seismograms. We then estimated the M_v values using individual high-pass-filtered vertical seismograms, and averaged these values to obtain the seismic magnitude for each event.

Using these procedures, we estimated the source locations and amplitudes as well as the magnitudes of VT earthquakes at Taal between May 2011 and July 2012. For the source location determinations, we used a 10-s sliding time window with a 5-s overlap for events that were observed by five or more stations. VT earthquakes occurred in the region surrounding the Volcano Island down to depths of several kilometers (Fig. 9a). The source amplitude time series (Fig. 9b) shows that the events of various sizes occurred during this observational period, and we found a linear relationship between the estimated seismic magnitudes and the logarithm of the source amplitudes (Fig. 10, circles).

We determined the hypocenters of four large events, for which onset arrivals were more reliably measurable, by using the hypocenter determination method of Benz et al. (1996) with traveltimes calculated with the 1D model (Table 1). We set the initial hypocenter at a depth of 5 km beneath the Main Crater Lake, and performed 10 iterations of the inversion to determine the hypocenter for each event. The root mean squares of the P -wave first-arrival-time residuals for these events are listed in Table 3. These hypocenters and the source locations determined by the ASL method (Fig. 11, squares

Table 3

Root mean squares of the P -wave first-arrival time residuals (RMS) for individual events (see hypocenter locations in Fig. 11).

Event date	RMS (s)
2011-05-31	0.096
2012-05-05	0.158
2012-05-15	0.042
2012-06-25	0.045

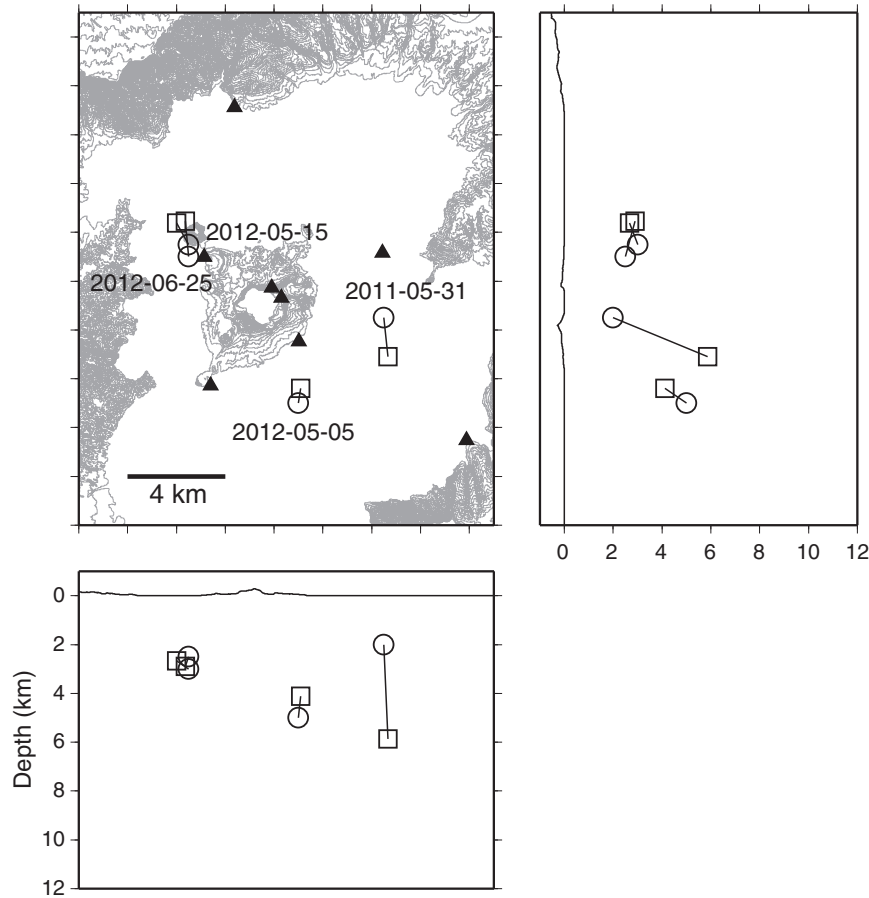


Fig. 11. Comparison of the source locations determined by the ASL method (circles) with hypocenters estimated from *P*-wave onset arrival time measurements (squares). The numbers indicate event dates.

and circles, respectively) correspond fairly well, although for one event the difference between them is relatively large, especially with regard to the depth estimate.

4.3. ASL analyses of LP events at Cotopaxi and explosion events at Tungurahua

We further applied the ASL method to LP events at Cotopaxi and explosion events at Tungurahua in Ecuador. Cotopaxi (elevation,

5876 m) is a large stratovolcano in the Eastern Cordillera of the Ecuadorian Andes. Several major eruptions with accompanying pyroclastic flows, ash falls, and lahars have occurred there since 1534 (Barberi et al., 1995; Mothes et al., 1998). Renewed seismic activity of Cotopaxi began in January 2001, and the VT and LP activity has remained high since then (Molina et al., 2008). Tungurahua (elevation, 5023 m) is an andesitic stratovolcano (Hall et al., 1999) and has continued its eruptive activity since 1999. Major eruptions accompanying pyroclastic flows occurred in July and August 2006 (Samaniego et al., 2011).

At each volcano, five seismic stations are maintained by the Instituto Geofísico, Escuela Politécnica Nacional (IG-EPN) of Ecuador. Each station is equipped with a broadband seismometer (Guralp CMG-40T, 0.02–60 s) and an infrasonic sensor (ACO 7144/4144, 0.01–10 s) with a 24-bit digitizer (Geotech Smart24D). The broadband sensor at each station was installed in the same manner as those at Taal volcano (Kumagai et al., 2010).

The observed waveforms of an LP event that occurred on 7 April 2012 at Cotopaxi are displayed in Fig. 12. This type of events has repetitively occurred beneath Cotopaxi without an eruptive activity. Molina et al. (2008) analyzed VLP/LP events at Cotopaxi in late June 2002 that produced similar waveforms and interpreted these signals to have been generated by gas-release processes from a dike intruded beneath Cotopaxi. In contrast, repeated explosive eruptions of Tungurahua volcano occurred during its active period. The observed seismic and infrasonic waveforms of one such event that occurred on 2 December 2011 are shown in Fig. 13.

We systematically determined the source locations and amplitudes along with the magnitudes of recent LP events at Cotopaxi and explosion events at Tungurahua by procedures similar to those used for the

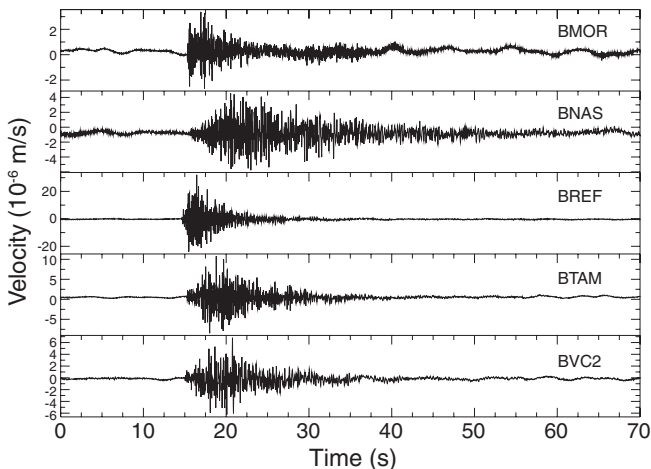


Fig. 12. Observed vertical seismograms of an LP event on 7 April 2012 at Cotopaxi volcano, Ecuador.

VT earthquakes at Taal volcano (see Section 4.2). Following Kumagai et al. (2010), in the first step (source location determinations), we used a frequency band of 7–12 Hz with site amplification corrections for the LP events at Cotopaxi and a frequency band of 5–10 Hz without site amplification corrections for the explosion events at Tungurahua. We used a homogeneous S-wave velocity of 2000 m/s and $Q = 60$ at both volcanoes (Kumagai et al., 2010). We did not correct site amplification factors for explosion events at Tungurahua because Kumagai et al. (2010) reported that the normalized residuals for an explosion event were smaller without the corrections. We also consider the use of a homogeneous structure to be justified because of the shallowness of these LP and explosion events as shown below. We used a sliding time window of 10 s with a 5-s overlap. For the explosion events at Tungurahua, we used time windows before the arrivals of the infrasonic waves, because the infrasonic waves were contaminated in the seismograms (see Fig. 13). In the second step, we used the reference frequency band of 5–10 Hz and $Q = 60$ at both volcanoes without site amplification corrections to estimate the source amplitudes.

The LP sources at Cotopaxi were located near the summit with a vertical elongation (Fig. 14). Waveform inversion of a VLP/LP event on 14 January 2009 pointed to a tensile crack source beneath the northeastern flank at a depth of 4 km above sea level (Kumagai et al., 2010). This location is consistent with those of the LP events determined by the ASL method (Fig. 14); the vertical elongation may be due to the effects of noise and limited depth resolution. We also found a scaling relation between seismic magnitudes and the estimated source amplitudes for these LP events (Fig. 10, squares).

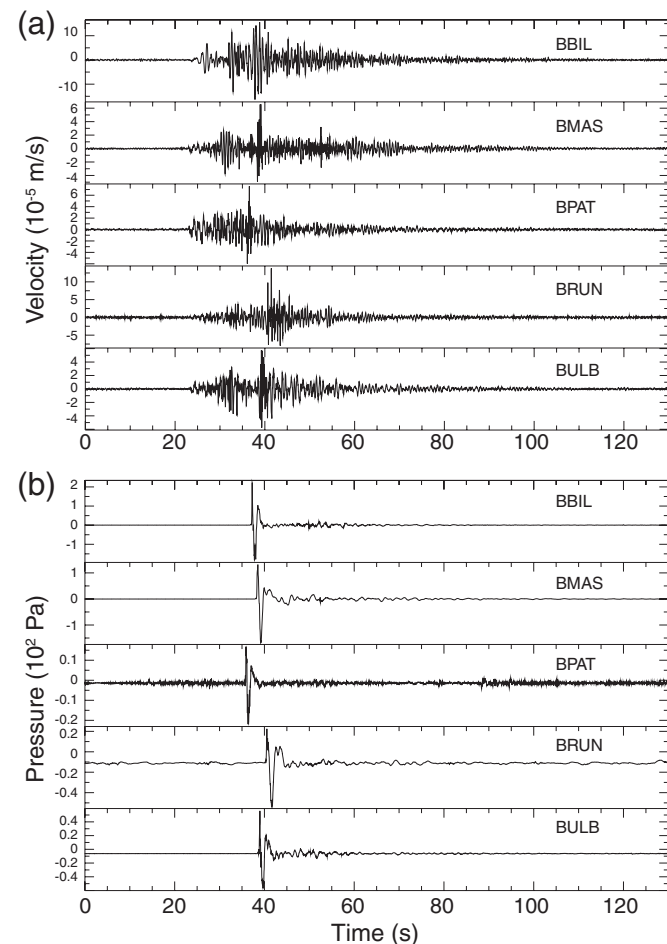


Fig. 13. (a) Observed vertical seismograms and (b) infrasonic waveforms of an explosion event on 2 December 2011 at Tungurahua volcano, Ecuador.

The source locations of the explosion events at Tungurahua were determined near the summit vent (Fig. 15), a location consistent with that of the explosion event reported by Kumagai et al. (2010). For an explosion event on 11 February 2010, Kumagai et al. (2011a) estimated an ascending source from a depth of 6 km below the summit of Tungurahua by using the ASL method with a 2-s time window. For this event, the source location with the largest source amplitude with a 10-s time window was also located near the summit (the result not shown here). The relation between the estimated magnitude and the logarithm of the source amplitude was also proportional for the explosion events at Tungurahua (Fig. 10, triangles).

5. Discussion

As demonstrated by our synthetic tests, source locations determined by the ASL method are not strongly affected by velocity structure and noise. As shown in Eq. (1), the amplitude decay as a function of source-station distance is the main factor influencing the determination of the source location, whereas the velocity structure or traveltimes may not seriously affect the source location determination, especially when local network data are used, as in this study. Our application of the ASL method to the largest VT earthquake at Taal confirmed this independence of the ASL results from the velocity structure model used. Moreover, by applying the ASL method, we were able to determine the source locations of even small VT earthquakes for which onset readings are difficult (Fig. 9).

On the other hand, the synthetic tests indicated that the ASL accuracy is dependent on site amplification factors (Fig. 4). The hypocenters of the large VT earthquakes at Taal, determined from onset arrival times, were basically consistent with their source locations determined by the ASL method, but for one event there was a relatively large difference in the depth estimate (Fig. 11). This difference may be attributable to errors in our estimation of the site amplification factors by the coda normalization method. The errors in the site amplification factors increased as the frequency band of the observations increased (Table 2). On the other hand, hypocenters determined by onset arrival times can be greatly affected by a highly heterogeneous volcano structure (e.g., Benz et al., 1996). Therefore, it would be difficult to conclude from the data presented in this study alone whether the hypocenter estimate or the ASL estimate is more appropriate.

Another important effect in the ASL method is the station coverage of the source. An artifact source location would appear when the source is located outside of the network (Kumagai et al., 2013). The spatial resolution of an estimated source location may be evaluated by the spatial distribution of residuals such as one shown in Fig. 8. If small residuals are not well constrained spatially in the residual distribution, an estimated source location should be considered to be unreliable.

The ASL method determines the source location and source amplitude simultaneously. We used a practical approach that could minimize the effect of station site amplifications in seismic networks at different volcanoes, and showed that a scaling relation exists between the seismic magnitude and source amplitude (Fig. 10). This relationship is not highly dependent on the event type, and is approximated by the equation

$$M_v = 1.10 \log A_s + 2.96, \quad (13)$$

where A_s is the source amplitude (m^2/s). The existence of a proportional relationship suggests that the source amplitude can be used as a quantitative measure of the size of various types of volcano-seismic events observed at different volcanoes. The seismic magnitude has been previously defined in various ways, and there existed the difficulty to compare it at different volcanoes. The source amplitude determined by the ASL method has a clear definition and physical basis in terms of the assumption of isotropic S-wave radiation in a reference frequency band of

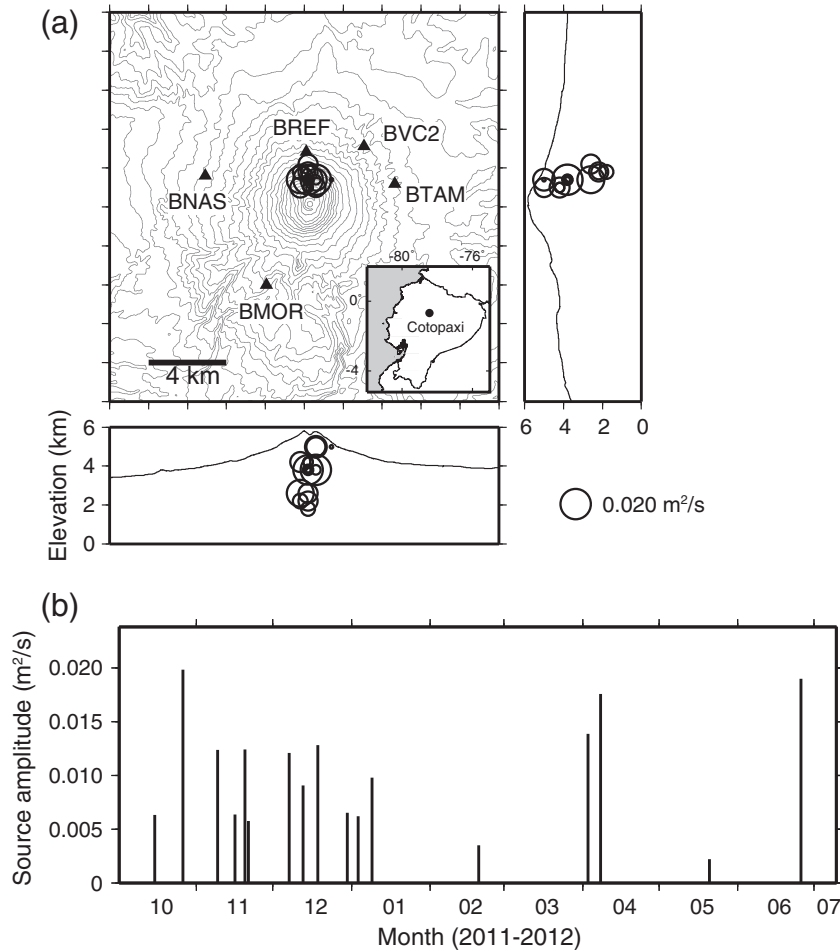


Fig. 14. (a) Source locations and source amplitudes of LP events at Cotopaxi volcano. The size of each circle represents the source amplitude, which is scaled to a reference circle outside the map. The inset shows the location of Cotopaxi volcano in Ecuador. (b) The source amplitude as a function of time between October 2011 and July 2012.

5–10 Hz. Moreover, the ASL method can be used to determine source locations of small events.

The reduced displacement (D_R) introduced by Aki and Koyanagi (1981) has been commonly used to quantify sources of tremor (e.g., Fehler, 1983; McNutt, 1992; Alparone et al., 2003; Benoit et al., 2003). Aki and Koyanagi (1981) defined D_R (units, m²) as the root-mean-square (RMS) displacement corrected for geometrical spreading and instrumental response:

$$D_R = Ar / (2\sqrt{2}), \quad (14)$$

where A is the peak-to-peak amplitude of tremor corrected for instrumental response at the tremor frequency and r is the source-station distance. The factor $2\sqrt{2}$ is used to obtain the RMS amplitude from the peak-to-peak amplitude under the assumption that tremor generates a sinusoidal signal.

In the ASL method, the source amplitude defined by Eq. (5) (units, m²/s), which is equivalent to the definitions of Battaglia and Aki (2003), Battaglia et al. (2005a, 2005b), and Kumagai et al. (2010), is estimated by using ground velocities corrected for instrumental response, geometrical spreading, and medium attenuation. Thus, the source amplitude is conceptually similar to the reduced displacement. Battaglia

et al. (2005b) discussed the relationship between the reduced displacement and source amplitude of tremor with a monochromatic sinusoidal signal. Our study showed that the source amplitude is a useful parameter for quantifying the source of various types of volcano-seismic signals. Thus, it provides a way to compare sizes of events occurring at different volcanoes. We define the source-amplitude magnitude (M_V) through Eq. (13) for volcano-seismic signals.

Source amplitude estimations may depend on station site conditions, so the applicability of Eq. (13) at other volcanoes must be confirmed in future studies. We used seismic data from seismometers installed in a similar way. To our knowledge, the way of the seismometer installation at Taal, Tungurahua, and Cotopaxi has been used at other volcanoes especially for broadband seismometers. Thus, it should be possible to compare the source amplitudes at such volcanoes with those estimated in this study. Furthermore, if the source location is known or can be reasonably assumed, it is possible to determine the source amplitude by using single-station data. This can be done by using vertical envelope amplitude band-pass filtered between 5 and 10 Hz and averaged over a 10-s window that includes the maximum amplitude. Then, a source amplitude compatible with those estimated in this study can be estimated by using Eq. (6) with $N = 1$ and assuming a typical Q value of 50. Determination of source amplitudes at many volcanoes will contribute to the establishment of a reliable quantitative measure of volcano-seismic event size. The ASL method can be easily automated and enables us to perform near real-time estimations of the source locations and amplitudes of

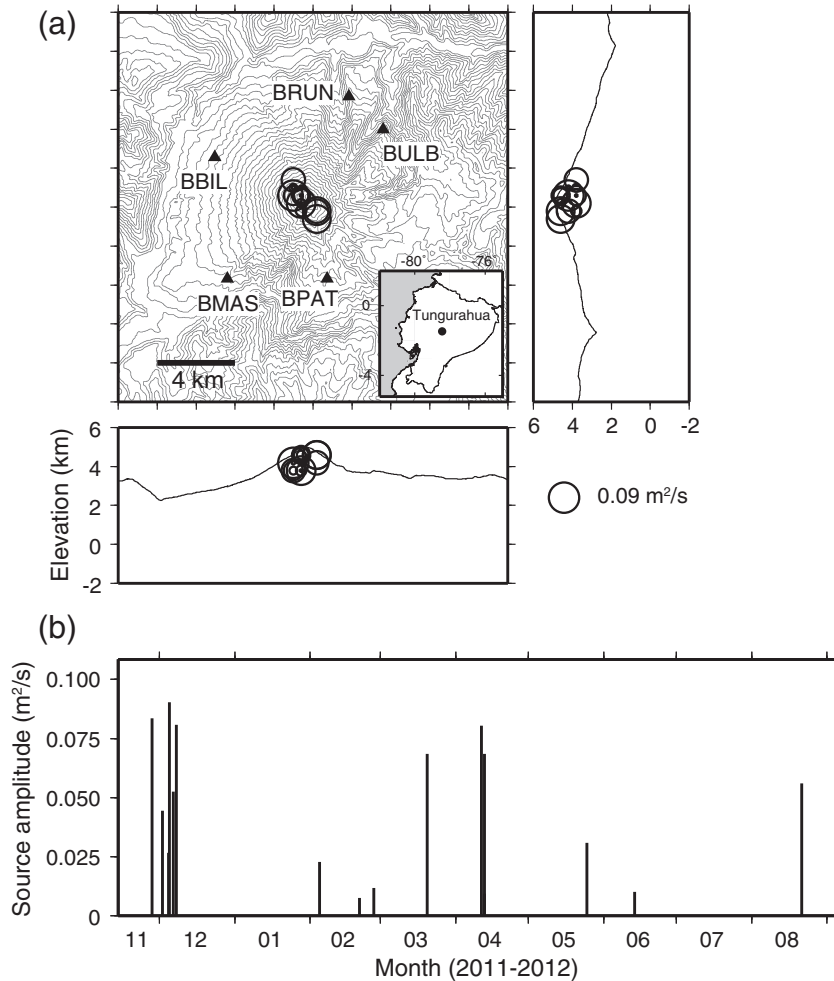


Fig. 15. (a) Source locations and source amplitudes of explosion events at Tungurahua volcano. The size of each circle represents the source amplitude, which is scaled to a reference circle outside the map. The inset shows the location of Tungurahua volcano in Ecuador. (b) The source amplitude as a function of time between November 2011 and August 2012.

volcano-seismic signals. Such information would contribute to the improved monitoring of active volcanoes.

6. Conclusions

We tested the ASL method by using synthetic seismograms calculated under the assumption of isotropic radiation of *S* waves. Our test results indicated that ASL results are not strongly dependent on velocity structure and noise, but are more affected by site amplification factors.

We analyzed VT earthquakes at Taal volcano, Philippines, where the seismic network consists of eight seismometers (five broadband and three short-period seismometers). We estimated station site amplification factors by the coda normalization method. Our ASL analysis of the largest VT earthquake indicated that a frequency band of 7–12 Hz and $Q = 50$ provided the minimum normalized residual. We proposed a two-step approach to estimate the source amplitude as follows: The source location is first determined by using a frequency band of 7–12 Hz and $Q = 50$ with site amplification corrections, and then the source amplitude is estimated by using waveform data at broadband seismic stations only without site amplification corrections and a reference frequency band of 5–10 Hz and $Q = 50$.

Using this two-step approach, we systematically applied the ASL method to VT earthquakes at Taal, and estimated their source locations

and amplitudes as well as seismic magnitudes. We similarly analyzed LP events at Cotopaxi and explosion events at Tungurahua. At all three volcanoes, we found a proportional relation between the magnitude and the logarithm of the source amplitude without any strong dependence on event type.

At these three volcanoes, all of broadband seismometers had been installed in a similar way, which may have minimized site effects. The source amplitude has a clear physical basis in terms of the assumption of isotropic *S*-wave radiation in a reference frequency band of 5–10 Hz. The ASL method can determine source locations of small events for which onset measurements are difficult, and thus can estimate the sizes of events over a wider range of sizes compared with conventional hypocenter determination approaches. The source amplitude determined by the ASL method may thus be a useful quantitative measure of volcano-seismic event size.

Acknowledgments

We thank the staff in Buco Volcano Observatory of the PHIVOLCS for installing and maintaining the Taal network. We also thank the IG-EPN members for maintaining the Cotopaxi and Tungurahua networks. Comments from Gilberto Saccorotti and Silvio De Angelis helped to improve the manuscript.

Appendix A. Source location determination

Kumagai et al. (2010) proposed that Eq. (6) is used to estimate the source amplitude. They mentioned that Eq. (6) was derived by minimizing E given by Eq. (8), but this statement may not be correct. Eq. (6) can be derived from the method of moments (e.g., Larsen and Marx, 2010) as follows. Using the observed (g_i^o) and calculated (g_{ij}) envelope amplitudes averaged over a time window T_w , we obtain the equation

$$g_i^o (t_s^k + \tau_{ij}) r_{ij} e^{C\tau_{ij}} - A_{jk} = \varepsilon_i, \tag{A1}$$

where ε_i represents observation errors. In accordance with the method of moments, we assume that the first moment (mean) of these errors is zero, which leads to Eq. (6). On the other hand, by the least-squares method, the observational equation is

$$g_i^o (t_s + \tau_{ij}) - A_{jk} \frac{1}{r_{ij}} e^{-C\tau_{ij}} = \varepsilon_i'. \tag{A2}$$

This leads to the least-squares estimation of A_{jk} as

$$A_{jk} = \frac{\sum_{i=1}^N y_{ij} g_i^o}{\sum_{i=1}^N y_{ij} y_{ij}}, \tag{A3}$$

where N is the number of stations and

$$y_{ij} = \frac{1}{r_{ij}} e^{-C\tau_{ij}}. \tag{A4}$$

Here, ε_i' is assumed to have a Gaussian distribution, but it is uncertain whether the assumption of a Gaussian distribution is always valid. In contrast, Eq. (6) does not require any assumption about the error distributions.

Fig. A1 plots the normalized residual distribution obtained by using the least-squares estimations of A_{jk} through Eq. (A3) for the largest VT earthquake at Taal and exactly the same parameters as those used to produce the spatial distribution of the normalized residuals in Fig. 8. The minimum residual positions in Figs. 8 and A1 nearly coincide (there is one node difference in the depth direction), but the residual distributions differ. Next, we plotted the error distribution at the minimum residual nodes (Figs. 8 and A1, stars) and at the source nodes denoted as S1 and S2 in Figs. 8 and A1, respectively. The error distributions at the minimum residual nodes obtained by using Eqs. (6) and (A3), respectively, resemble a Gaussian distribution (Fig. A2a and c). The error distribution at node S2 obtained with Eq. (A3) is also a Gaussian-like distribution (Fig. A2d), but that at node S1 obtained by using Eq. (6) is non-Gaussian (Fig. A2b). These results suggest that the assumption of a Gaussian error distribution may not always be valid, thus justifying the use of Eq. (6) based on the method of moments.

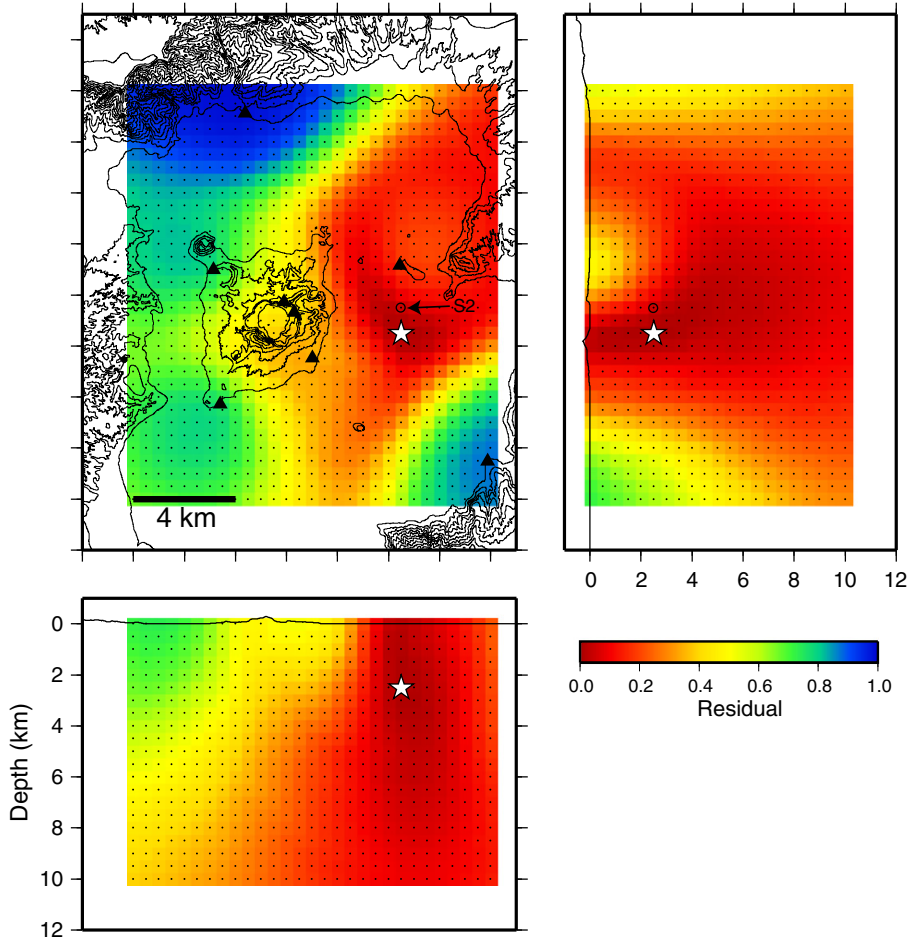


Fig. A1. Normalized residual distributions for the VT earthquake on 31 May 2011 at Taal (see Fig. 6) obtained with Eq. (A3) based on a least-squares solution. Stars indicate the minimum residual location.

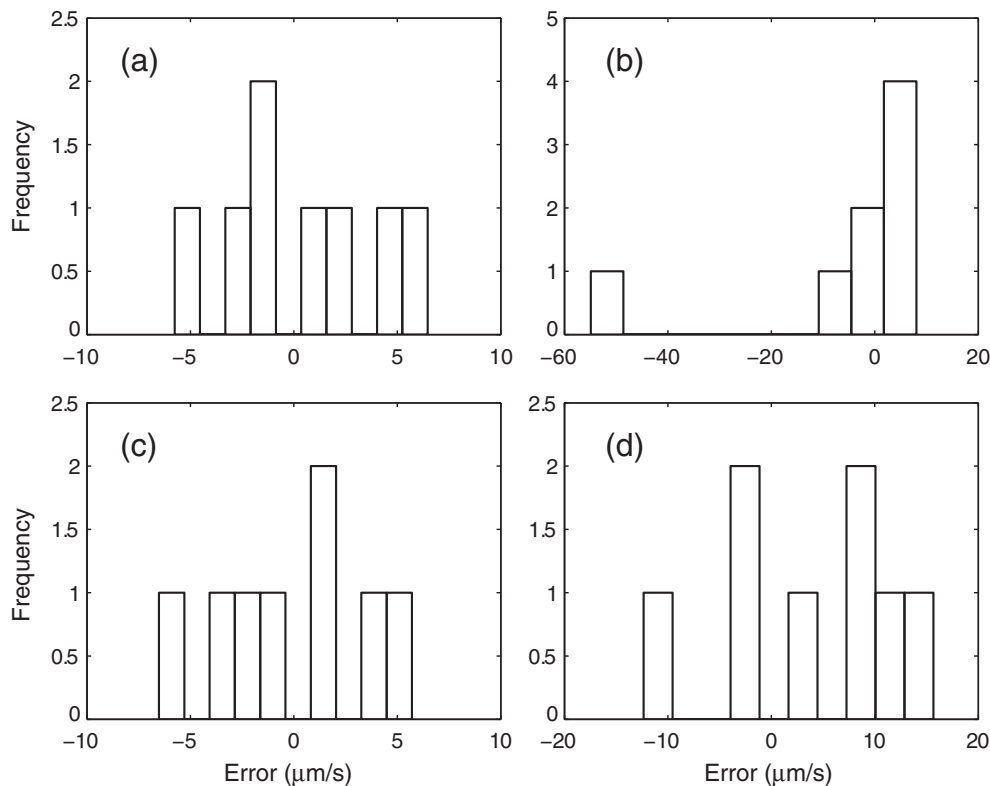


Fig. A2. Observation error distributions at the minimum residual locations in (a) Fig. 8 and (c) Fig. A1 and at the source nodes (b) S1 (Fig. 8a) and (d) S2 (Fig. A1).

References

- Aki, K., Koyanagi, R., 1981. Deep volcanic tremor and magma ascent mechanism under Kilauea, Hawaii. *Journal of Geophysical Research* 86, 7095–7109.
- Alparone, S., Andronico, D., Lodato, L., SgROI, T., 2003. Relationship between tremor and volcanic activity during the Southeast Crater eruption on Mount Etna in early 2000. *Journal of Geophysical Research* 108, 2241. <http://dx.doi.org/10.1029/2002JB001866>.
- Barberi, F., Coltelli, M., Frullani, A., Rosi, M., Almeida, E., 1995. Chronology and dispersal characteristics of recently (last 5000 years) erupted tephra of Cotopaxi (Ecuador): implications for long-term eruptive forecasting. *Journal of Volcanology and Geothermal Research* 69, 217–239.
- Battaglia, J., Aki, K., 2003. Location of seismic events and eruptive fissures on the Piton de la Fournaise volcano using seismic amplitudes. *Journal of Geophysical Research* 108, 2364. <http://dx.doi.org/10.1029/2002JB002193>.
- Battaglia, J., Got, J.-L., Okubo, P., 2003. Location of long-period events below Kilauea Volcano using seismic amplitudes and accurate relative relocation. *Journal of Geophysical Research* 108, 2553. <http://dx.doi.org/10.1029/2003JB002517>.
- Battaglia, J., Aki, K., Ferrazzini, V., 2005a. Location of tremor sources and estimation of lava output using tremor source amplitude on the Piton de la Fournaise volcano: 1. Location of tremor sources. *Journal of Volcanology and Geothermal Research* 147, 268–290.
- Battaglia, J., Aki, K., Staudacher, T., 2005b. Location of tremor sources and estimation of lava output using tremor source amplitude on the Piton de la Fournaise volcano: 2. Estimation of lava output. *Journal of Volcanology and Geothermal Research* 147, 291–308.
- Benoit, J.P., McNutt, S.R., Barboza, V., 2003. Duration–amplitude distribution of volcanic tremor. *Journal of Geophysical Research* 108, 2146. <http://dx.doi.org/10.1029/2001JB001520>.
- Benz, H.M., Chouet, B.A., Dawson, P.B., Lahr, J.C., Page, R.A., Hole, J.A., 1996. Three-dimensional *P* and *S*-wave velocity structure of Redoubt Volcano, Alaska. *Journal of Geophysical Research* 101, 8111–8128.
- Chouet, B., 1996. Long-period volcano seismicity: its source and use in eruption forecasting. *Nature* 380, 309–316.
- Chouet, B.A., Matoza, R.S., 2013. A multi-decadal view of seismic methods for detecting precursors of magma movement and eruption. *Journal of Volcanology and Geothermal Research* 252, 108–175.
- Fehler, M., 1983. Observations of volcanic tremor at Mount St. Helens Volcano. *Journal of Geophysical Research* 88, 3476–3483.
- Hall, M.L., Robin, C., Beate, B., Mothes, P., Monzier, M., 1999. Tungurahua Volcano, Ecuador: structure, eruptive history and hazards. *Journal of Volcanology and Geothermal Research* 91, 1–21.
- Kawakatsu, H., Yamamoto, M., 2007. Volcano seismology. In: Kanamori, H., Schubert, G. (Eds.), *Treatise on Geophysics: Earthquake Seismology*, vol. 4. Elsevier, New York, pp. 389–420.
- Kumagai, H., Nakano, M., Maeda, T., Yepes, H., Palacios, P., Ruiz, M., Arrais, S., Vaca, M., Molina, I., Yamashina, T., 2010. Broadband seismic monitoring of active volcanoes using deterministic and stochastic approaches. *Journal of Geophysical Research* 115, B08303. <http://dx.doi.org/10.1029/2009JB006889>.
- Kumagai, H., Palacios, P., Ruiz, M., Yepes, H., Kozono, T., 2011a. Ascending seismic source during an explosive eruption at Tungurahua volcano, Ecuador. *Geophysical Research Letters* 38, L01306. <http://dx.doi.org/10.1029/2010GL045944>.
- Kumagai, H., Saito, T., O'Brien, G., Yamashina, T., 2011b. Characterization of scattered seismic wavefields simulated in heterogeneous media with topography. *Journal of Geophysical Research* 116, B03308. <http://dx.doi.org/10.1029/2009JB007718>.
- Kumagai, H., Pulido, N., Fukuyama, E., Aoi, S., 2013. High-frequency source radiation during the 2011 Tohoku-Oki earthquake, Japan, inferred from KIK-net strong-motion seismograms. *Journal of Geophysical Research* 118, 1–18. <http://dx.doi.org/10.1029/2012JB009670>.
- Larsen, R.J., Marx, M.L., 2010. *An Introduction to Mathematical Statistics and Its Applications*, fifth edition. Prentice Hall, New Jersey 757.
- McNutt, S.R., 1992. Volcanic tremor. *Encyclopedia of Earth System Science*, vol. 4. Academic Press, San Diego 417–425.
- McNutt, S.R., 2005. Volcanic seismology. *Annual Review of Earth and Planetary Sciences* 32, 461–491.
- Molina, I., Kumagai, H., García-Aristizábal, A., Nakano, M., Mothes, P., 2008. Source process of very-long-period events accompanying long-period signals at Cotopaxi Volcano, Ecuador. *Journal of Volcanology and Geothermal Research* 176, 119–133.
- Mothes, P.A., Hall, M.L., Janda, R.J., 1998. The enormous Chillón Valley Lahar: an ash-flow-generated debris flow from Cotopaxi Volcano, Ecuador. *Bulletin of Volcanology* 59, 233–244.
- Neuberg, J., 2000. Characteristics and causes of shallow seismicity in andesite volcanoes. *Philosophical Transactions of the Royal Society of London. Series A* 358, 1533–1546.
- Ogiso, M., Yomogida, K., 2012. Migration of tremor locations before the 2008 eruption of Meakandake volcano, Hokkaido, Japan. *Journal of Volcanology and Geothermal Research* 217–218, 8–20.
- Phillips, W.S., Aki, K., 1986. Site amplification of coda waves from local earthquakes in central California. *Bulletin of the Seismological Society of America* 76, 627–648.
- Podvin, P., Lecomte, I., 1991. Finite difference computation of traveltimes in very contrasted velocity models: a massively parallel approach and its associated tools. *Geophysical Journal International* 105, 271–284.
- Samaniego, P., Le Penec, J.-L., Robin, C., Hidalgo, S., 2011. Petrological analysis of the pre-eruptive magmatic process prior to the 2006 explosive eruptions at Tungurahua volcano (Ecuador). *Journal of Volcanology and Geothermal Research* 199, 69–84.
- Takemura, S., Furumura, T., Saito, T., 2009. Distortion of the apparent *S*-wave radiation pattern in the high-frequency wavefield: Tottri-Ken Seibu, Japan earthquake of

2000. *Geophysical Journal International* 178, 950–961. <http://dx.doi.org/10.1111/j.1365-246X.2009.04210.x>.
- Vidale, J., 1990. Finite-difference calculation of travel times in three dimensions. *Geophysics* 55, 521–526.
- Watanabe, H., 1971. Determination of earthquake magnitude at regional distance in and near Japan. *Zisin, Second Series* 24, 189–200.
- Yamasato, H., 1997. Quantitative analysis of pyroclastic flows using infrasonic and seismic data at Unzen Volcano, Japan. *Journal of Physics of the Earth* 45, 397–416.
- Zobin, V., 2012. *Introduction to Volcanic Seismology*, 2nd edition. Elsevier.